Characterization of poly(1,4-phenyleneterephthalamide) in concentrated sulphuric acid: 1. Static and dynamic properties

Qicong Ying and Benjamin Chu*
Department of Chemistry, and Department of Materials Science and Engineering, State University of New York at Stony Brook, Long Island, New York, 11794-3400, USA*

and Renyuan Qian, Jingsheng Bao, Jiyu Zhang and Chaochou Xu
Institute of Chemistry, Academia Sinica, Beijing, Peoples Republic of China
(Received 7 June; revised 6 September 1984)

Laser light scattering including angular dependence of total integrated scattered intensity and of the spectral distribution has been used to characterize five samples of poly(1,4-phenylene terephthalamide), PPTA (commercially known as Kevlar), of different molecular weights in 96% sulphuric acid and 0.1 N K_2SO_4. The data are supplemented by intrinsic viscosity measurements used to detect the possible effects of association, by differential refractometry providing a measure of the refractive index increments in mixed solvents (H_2O, H_2SO_4 and K_2SO_4) and by spectrophotometry for the extinction coefficient needed in the correction of attenuation in light scattering studies. The results show $\langle D \rangle_z = 2.11 \times 10^{-5} \bar{M}_w^{-0.75}$ cm^2 s^{-1} in reasonable agreement with an average of many of the published intrinsic viscosity data obeying $[\eta] = 1.09 \times 10^{-3} M_w^{1.25}$ ml g^{-1} and M_w expressed in g mol^{-1}.

(Keywords:

INTRODUCTION

Poly(1,4-phenylene terephthalamide) (PPTA) fibres with high tenacity and modulus can be obtained by spinning from its anisotropic liquid-crystalline solutions. PPTA, or Kevlar[3], fibres are inherently flame resistant, do not melt, and have a useful wide temperature range from -196°C to 200°C. The fibre has a density of 1.44 g cm^{-3} and a tensile strength of 2.76×10^3 MPa whereas stainless steel has a density of 7.83 g cm^{-3} and a tensile strength of 1.72×10^3 MPa. Since their discovery in the mid-1960s, PPTA fibres found a multitude of applications in replacing steel, fibre glass, asbestos and aluminium for aircraft/aerospace, marine and general industrial uses. One of its most well-known applications is in the personnel protection field, such as the bullet-proof vest. PPTA forms a hybrid composite with graphite fibres and is destined to be an important component in future polymer composites where weight and strength are important factors.

However, the characterization of *para*-aromatic polyamides has often been a difficult task. For example, PPTA is soluble mainly in corrosive strong protic (sulphonic) acids, such as methane sulphonic acid, chlorosulphonic acid, or concentrated sulphuric acid. The corrosive nature of these solvents demands special modifications to analytical instrumentation, especially for gel permeation chromatography. Therefore, it is usually quite difficult to obtain quantitative and absolute characterizations of PPTA dissolved in sulphonic acids.

Although PPTA was discovered almost 20 years ago and Kevlar fibres have found many unique applications, no absolute method for molecular characterizations of PPTA exists. In a series of two articles, we want to report: 1: static and dynamic properties of dilute solutions of PPTA from measurements of intrinsic viscosity, light scattering intensity and linewidth in concentrated sulphuric acid, and 2: determinations of molecular weight distributions of PPTA based on recent developments in correlation function profile analysis. A preliminary account of this development has been reported[4].

Solution properties of some rod-like polymers, including PPTA[5-7], have been investigated extensively by Berry and coworkers[5-12]. Molecular characterizations of PPTA using light scattering and viscometry in dilute solutions showed the polymer to have a rod-like conformation and to be prone to interchain aggregation[5]. Further studies in dilute solutions of rod-like macro-ions revealed that polymers, such as poly(1,4-phenylene-2,6-benzobisthiazole) (PBT), could be associated even at very high dilution, probably in metastable aggregates. Lee *et al.*[7] also suggested that the formation of metastable aggregates does not imply unusually large attractive interactions among the rod-like chains. However, effects of electrostatic interactions increase in range with decreasing ionic strength of the solvent but have little influence on chain conformation, owing to the large persistence length with $\rho \approx 45$ nm for PPTA in solvents at moderately high ionic strength. Although PPTA appears to be soluble in dimethylacetamide (DMAC) and other amide solvents[13], aggregation is a serious problem. Therefore, only concentrated sulphuric acid in the presence of K_2SO_4 as the added salt was considered here. Protonation of PPTA invariably alters the electrostatic forces which play a very important role in the dissolution and possible metastable aggregation of PPTA even in dilute solution. Our characterization of PPTA in a strong

0032-3861/85/091401-07$03.00

acid in the presence of added salt undoubtedly deals with a slightly modified form of PPTA in solution where the Debye screening length κ^{-1} is relatively small and where we have assumed negligible chemical modification of PPTA by the strong acid.

THEORETICAL BACKGROUND

Light-scattering integrated intensity

For worm-like chains, measurements of light-scattering integrated intensity in dilute solution as a function of concentration, C, and scattering angle, θ, provide information on the weight average molecular weight M_w, the z-average root-mean-square radius of gyration $\langle R_g^2 \rangle_z^{0.5}$, the molecular anisotropy, δ, and the second virial coefficient, A_2, by analysis of the vertical and horizontal components, R_{VV} and R_{HV}, of the Rayleigh ratio using vertically polarized incident light[7]:

$$\lim_{\theta \to 0}\left(\frac{HC}{R_{VV}}\right)^{1/2} = \left(\frac{HC}{R_{VV}}\right)_0^{1/2}\left(1 + \frac{A_2 M_w}{(1+4/5\delta^2)}C + \cdots\right) \quad (1)$$

$$\lim_{\theta \to 0}\frac{HC}{R_{HV}} \simeq \left(\frac{HC}{R_{HV}}\right)_0 + 0(C^2) \quad (2)$$

where:

$$\left(\frac{HC}{R_{VV}}\right)_0 = \lim_{\substack{\theta \to 0 \\ C \to 0}} \frac{HC}{R_{VV}}$$

and

$$\left(\frac{HC}{R_{VH}}\right)_0 = \lim_{\substack{\theta \to 0 \\ C \to 0}} \frac{HC}{R_{HV}}$$

$$\lim_{C \to 0}\frac{R_{VV}}{HCM} = (1 + 4/5 \cdot \delta^2) - 1/3[1 - 4/5\, f_1\delta + 4/7(f_2\delta)^2]u + \ldots, \quad (3)$$

$$\lim_{C \to 0}\frac{R_{HV}}{HCM} = 3/5\delta^2 - 9/35(f_3\delta)^2 u + \cdots, \quad (4)$$

where the optical constant $H = 4\pi^2 n^2 / N_A \lambda_0^4 (\partial n/\partial C)^2$, $K = 4\pi n/\lambda_0 \sin(\theta/2)$, and $u = R_g^2 K^2$. The functions f_i (discussed in reference 8) and the molecular anisotropy δ depend on the ratio ρ/L of the persistence length ρ and contour length $L(=M/M_L)$ with M_L being the mass per unit length along the chain contour[8]. $L/\rho = 0$ for rigid rods and becomes larger for coil-like polymers while $f_i \simeq 1$ for rod-like chains. In the absence of aggregation:

$$\left(\frac{R_{VH}}{R_{VV}}\right)_0 = \frac{3\delta^2}{5 + 4\delta^2} \quad (5)$$

Experimentally, by making measurements of R_{VV} and R_{HV} as a function of K and C, we get:

$$M_w: \left(\frac{HC}{R_{VV}}\right)_0 = \frac{1}{M_{app}} = \frac{1}{M_w(1 + 4/5\delta^2)} \quad (6)$$

$$R_g: \lim_{C \to 0}\frac{HC}{R_{VV}(u)} = \frac{1}{M_{app}}\left(1 + \frac{R_{g,app}^2 K^2}{3} + \ldots\right) \quad (7)$$

with:

$$R_g^2 = \frac{1 + 4/5\delta^2}{1 - 4/5\delta + 4/7\delta^2} R_{g,app}^2 \quad (8)$$

$$A_2: \lim_{\theta \to 0}\left(\frac{HC}{R_{VV}}\right)^{-1} = (1 + 4/5\delta^2)M_w - 2A_2 M_w^2 C + O(C^2) \quad (9)$$

$$\delta: \lim_{\theta \to 0}\left(\frac{HC}{R_{HV}}\right)^{-1} \simeq 3/5\delta^2 M_w - O(C^2) \quad (10)$$

and equation (5). With the worm-like chain model the observable quantities M_w, $R_g (\equiv \langle R_g^2 \rangle_z^{0.5})$, A_2 and δ are described in terms of ρ, L and M. With known value of ρ, we can then estimate δ_0 [14-18]:

$$\delta^2 = \delta_0^2 Y(L/\rho) \quad (11)$$

where:

$$Y(Z = L/\rho) = (2/(3Z))\{1 - (3Z)^{-1}[1 - e^{-3Z}]\}, \quad (12)$$

$$R_g^2 = (L^2/12)W(L/\rho) \quad (13)$$

where:

$$W(Z) = (4/Z)[1 - 3Z^{-1} + 6Z^{-2} - 6Z^{-3}(1 - e^{-Z})] \quad (14)$$

Light-scattering intensity correlation

Photon correlation spectroscopy measures the intensity time correlation function $G^{(2)}(\tau)$ which can be related to the first-order electric field correlation function $g^{(1)}(\tau)$ by:

$$G^{(2)}(\tau) = A(1 + \beta|g^{(1)}(\tau)|^2) \quad (15)$$

in the self-beating mode where A is the background and β is a spatial coherence factor usually taken as an adjustable parameter in the data fitting procedure. We have analysed the net, measured, self-beating autocorrelation function:

$$G_{net}^{(2)}(\tau) = A\beta|g^{(1)}(\tau)|^2$$

using the cumulants method[19] and the singular value decomposition technique[20,21]. The cumulants method is used only to estimate the magnitude of the mean characterestic linewidth $\bar{\Gamma}$ and of its variance $(\mu_2/\bar{\Gamma}^2)$ defined by $\Gamma = \int \Gamma G(\Gamma)\,d\Gamma$ and $\mu_2 = \int (\Gamma - \Gamma)^2 G(\Gamma)\,d\Gamma$ with $G(\Gamma)$ being the normalized linewidth distribution function. In the cumulants expansion, we have:

$$g^{(1)}(\tau) \simeq \exp\left[-\bar{\Gamma}\tau + \Sigma(-1)^i \frac{\mu_i \tau^i}{i!}\right] \quad (16)$$

where, for $\mu_2/\bar{\Gamma}^2 \gtrsim 0.3$ and $\bar{\Gamma}\tau_{max} \simeq 3$ with τ_{max} being the τ value at the last correlator channel, we need $i = 4$ or 5 in the summation of equation (16) to obtain an appropriate estimate of $\bar{\Gamma}$.

The second method of analysis is the singular value decomposition technique which has been described briefly elsewhere[20]. Detailed implications are considered in the second paper. It is sufficient to outline here that we restrict $G(\Gamma)$ to the discrete multiple-exponential approximation, as expressed by:

$$G(\Gamma) = \sum_{i=1}^{N} P_i \delta(\Gamma - \Gamma_i) \quad (17)$$

where the Γ_i's are fixed but need not be equally spaced and the P_i's are the amplitude factors obtained by a linear least-squares fitting to the data. The singular value decomposition technique evaluates the P_i's in terms of a limited number of base functions. The larger singular values represent information elements which can be extracted from the noise level of the measured data. As the singular values decrease toward zero, the information elements below the noise level are then truncated. The

Table 1 Physical properties of PPTA in 96% H_2SO_4, with or without K_2SO_4

Sample No. designation	Condition 96% H_2SO_4 plus	$[\eta]$ (10^2 ml g^{-1})	M_w† (10^4 g mol^{-1})	A_2 (10^{-3} cm^3 mol g^{-2})	$\langle R_g^2 \rangle_z^{1/2}$ (nm)	δ
1	No K_2SO_4	1.16*	1.45	5.83	–	0.27
2	No K_2SO_4	2.25	1.59	3.70	–	0.31
3	No K_2SO_4	4.66	2.27	2.31	22	0.27
4	No K_2SO_4	5.72	3.84	2.81	33	0.21
	0.005 M K_2SO_4	–	3.03	3.48	28	0.25
	0.05 M K_2SO_4	–	2.98	3.90	33	0.26
5	No K_2SO_4	5.75*	4.83	2.46	48	0.22
	0.05 M K_2SO_4	–	4.42	3.12	36	0.26
	0.05 M K_2SO_4	–	4.26	3.23	35	0.20

* $\eta_{inh} = \frac{\ln \eta_r}{C}$ where η_r is the relative viscosity

† Estimated precision: ±5%

range of $G(\Gamma)$ is determined from the behaviour of the best solutions using a minimum number of base functions and satisfying the positivity constraint, i.e., the characteristic linewidth distribution cannot be negative. We have also analysed the intensity–intensity autocorrelation function $G^2(\tau)$ using the method of regularization[22]. Again, the details are discussed in the second paper. However, it should be noted that all appropriate methods of data analysis including the cumulants method are able to provide correct values for the mean characteristic linewidth. So, measurements of the z-average translational diffusion coefficient $\langle D \rangle_z$ which obey the scaling relation:

$$\langle D \rangle_{z,0} = k_D \bar{M}_w^{\alpha} D \tag{18}$$

at infinite dilution are independent of the method of data analysis. Equation (18) cannot hold for worm-like chains over large ranges of molecular weight since the persistence length for a specific polymer solution system remains constant. Therefore, at low molecular weights PPTA could start as stiff rods, while at very high molecular weights the polymer should have an extended chain behaviour implying that the scaling exponent α_D changes over the transition range from rigid rod to coil. However, over short but practical ranges of molecular weight in the transition region for worm-like chains, a log–log plot of D vs. M is likely to yield an effective scaling exponent whose value reflects the semi-rigid property of the polymer under the specific solution and temperature conditions.

EXPERIMENTAL

Material: poly(1,4-phenyleneterephthalamide) synthesis

Poly(1,4-phenyleneterephthalamide) (PPTA) was prepared by addition of terephthaloyl chloride (melting point 83°C–84°C) to 1,4-phenylenediamine (melting point 140°C–141°C) dissolved in a mixture of hexamethyl phosphoramide and dimethyl acetamide at ≈3°C. Five different molecular weight samples of PPTA with intrinsic viscosities varying from 1–6 × 10^2 ml g^{-1} in 96% H_2SO_4 were synthesized at the Institute of Chemistry in Beijing.

Preparation of solutions

Solutions at different concentrations were prepared individually by dissolving known weights of the dried PPTA in centrifuged (96%) concentrated sulphuric acid (Reagent ACS, Fisher Scientific Company) with or without added salt (K_2SO_4) in a volumetric flask. After dissolution of PPTA, the solution was centrifuged at ≈9000 rpm (≈9800 gravity) for 1–3 h before the middle portion of the centrifuged solution was transferred to the Teflon-capped, 10 mm o.d., light-scattering cell. Each preparation was then individually checked for the presence of large dust particles by viewing with a low powered HeNe laser beam with $\lambda_0 = 632.8$ nm at relatively small scattering angles (say, $\theta \lesssim 30°$). Filtration was not used for the PPTA solutions since the effects of possible aggregation were uncertain. Furthermore, we wanted to take a more cautious step for handling rod-like polymers in solution. So, only centrifugation was used to clarify the PPTA solutions. All measurements were completed within a few days after solution preparation although we found this precaution to be essentially unnecessary.

Methods of measurement

The intrinsic viscosity $[\eta]$ was determined at 30°C with an Ubbelohde viscometer using procedures similar to those reported elsewhere[6]. Only measurements at very low shear rates exhibiting Newtonian behaviour were used.

The extinction coefficient, ν, was determined using a standard double-beam spectrophotometer. The small cone of scattered light entering the transmitted beam in standard spectrophotometers usually yields an effective extinction coefficient with:

$$\gamma = I_0/I_t = e^{\nu C d} \tag{19}$$

where I_t and I_0 are the transmitted and the incident beam intensity, respectively; ν(cm^2 g^{-1}) is a concentration independent extinction coefficient, d is the length of light path (cm), and C is the concentration (g cm^{-3}). The refractive index increment (dN/dC) was determined using a Brice–Phoenix differential refractometer.

The light scattering apparatus has been described elsewhere[24]. We used a Spectra-Physics Model 165 argon ion laser operating, nominally, below 100 mW. In view of the absorption problem associated with PPTA solutions, some preliminary light scattering measurements were performed using $\lambda_0 = 488.0$ nm with different incident laser power (~50 mW–200 mW) and $\lambda_0 = 632.8$ nm from a Spectra-Physics Model 125 HeNe laser light (≈40 mW). We observed essentially the same results and, therefore, $\lambda_0 = 488.0$ nm was used for all studies. Intensity measurements were accumulated automatically every 10° between the scattering angles θ, of 35° and 140° for 10 s periods without the gating arrangement to exclude the effect of dust contributions because we did not want to include any

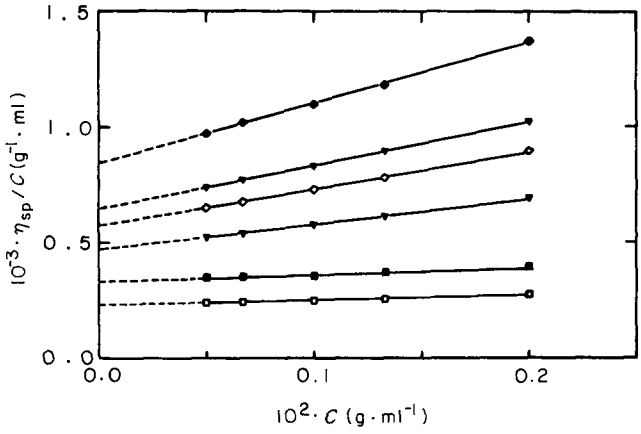

Figure 1 Plots of η_{sp}/C vs. C. Hollow symbols denote 96% H_2SO_4 as solvent and solid symbols denote 99.8% H_2SO_4 as solvent. □, ■, sample 2; ▽, ▼, sample 3; and ◇, ◆, sample 4. The physical properties of various PPTA samples are listed in *Table 1*

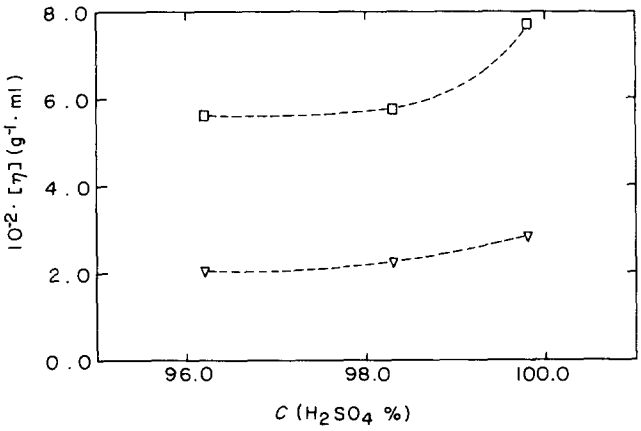

Figure 2 Effect of H_2O on the intrinsic viscosity of PPTA in concentrated sulphuric acid. □, sample 4; ▽, sample 2, as listed in *Table 1*

preconceived bias in our light-scattering integrated intensity measurements.

Correlation function measurements were made using a 96-channel single-clipped Malvern correlator. We accepted only those time correlation function measurements whose measured baseline corresponding to $G_k^{(2)}(\tau\rightarrow\infty)$ agreed with the computed baseline, defined by $A=\langle n_k\rangle\langle n\rangle N_S$ where $\langle n_k\rangle$, $\langle n\rangle$ and N_S are, respectively, the mean clipped count per sample time, the unclipped count per sample time, and the total number of samples with k being the clipping level. The reasonable agreement between the measured and the computed baselines, however, does not necessarily exclude an experimental difficulty on solution clarification of macroions, such as PPTA dissolved in concentrated sulphuric acid. We must always be careful of the possible complications of polar solvents, which are more difficult to clarify, and of electrostatic interactions which may cause aggregation. The light-scattering spectrometer was calibrated using benzene and NBS-705 polystyrene standard in cyclohexane.

RESULTS

Viscosity measurements

Figure 1 shows plots of η_{sp}/C vs. concentration for PPTA in 99.8% H_2SO_4 (filled symbols) and in 96.2% H_2SO_4 (hollow symbols) where the specific viscosity $\eta_{sp}=(\eta-\eta_s)/\eta_s$ with η and η_s being the viscosity of the solution and the solvent viscosity, respectively. No kinetic energy corrections were necessary because of the long flow times used. The intrinsic viscosity corresponds to η_{sp}/C at infinite dilution. A summary of measured intrinsic viscosities for the five PPTA samples using 96.2% H_2SO_4 as the solvent is listed in *Table 1*.

In view of possible molecular aggregation, we determined the concentration dependence of $[\eta]$ on H_2SO_4 content, as shown in *Figure 2*. The lower value of $[\eta]$ levels off when H_2SO_4 contains a small amount of water. 96% H_2SO_4 was selected as a solvent. To test the effect of ionic strength, K_2SO_4 was also added to the PPTA solution containing 96% H_2SO_4 and the molecular weight, the radius of gyration as well as the second virial coefficient of two PPTA samples (4 and 5) were determined.

Light-scattering measurements

The refractive index change as a function of concentration for PPTA (sample 2) in 96% H_2SO_4+0.5 M K_2SO_4 is shown in *Figure 3*. The refractive index increment is essentially independent of small changes of K_2SO_4 concentration suggesting negligible preferential absorption of additional sulphate ions. Therefore, we have not dialysed the PPTA solution which would have been difficult because of the presence of concentrated sulphuric acid. Δn at $\lambda_0=488$ nm was interpolated to be $3.53\times10^{-4}C$ [mg ml^{-1}].

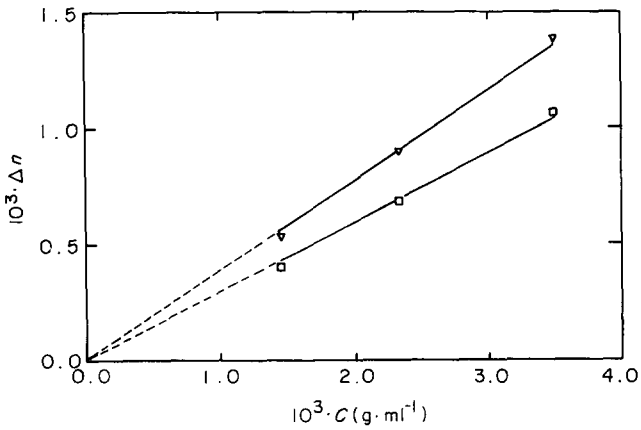

Figure 3 Concentration dependence of refractive index change of PPTA (sample 2) in 96% H_2SO_4+0.05 M K_2SO_4 at 30°C. ▽, $\lambda_0=436$ nm with $\Delta n=3.95\times10^{-4}C$ and C expressed in mg ml^{-1}; □, $\lambda_0=546$ nm with $\Delta n=3.06\times10^{-4}C$

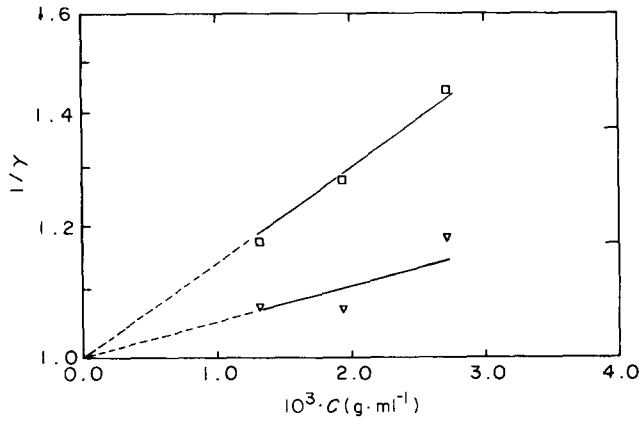

Figure 4 Plots of ln $1/\gamma$ vs. concentration with the extinction coefficient $\nu=1.7\times10^2$ and $6.3\times10\,cm^2\,g^{-1}$ for $\lambda_0=488$ and 632.8 nm, respectively. □, $\lambda_0=488$ nm; ▽, $\lambda_0=632.8$ nm

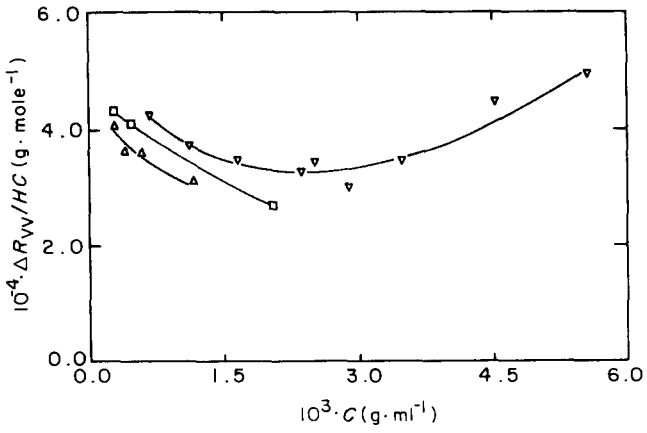

Figure 5 Plots of $\Delta R_{VV}/HC$ vs. concentration for sample 5. ▽, 96% H_2SO_4; □, 96% H_2SO_4 + 0.005 M K_2SO_4; △, 96% H_2SO_4 + 0.05 M K_2SO_4 ($\Delta R_{VV} = \lim_{K\to 0} Rvv$). The symbol △ is introduced to emphasize excess Rayleigh ratio where the solvent-scattered intensity has been subtracted from the solution scattered intensity. According to equations (6) and (9), the intercept should yield an apparent molecular weight M_{app} which appears to vary slightly with the solvent composition

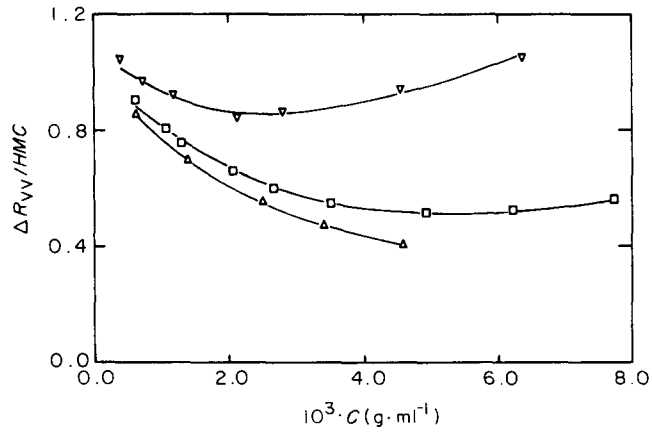

Figure 6 Plots of $\Delta R_{VV}/HMC$ vs. concentration for sample 4. ▽, 96% H_2SO_4; □, 96% H_2SO_4 + 0.005 M K_2SO_4; △, 96% H_2SO_4 + 0.05 M K_2SO_4. $\Delta R_{VV} = \lim_{K\to 0} Rvv$ with △ signifying excess Rayleigh ratio. With comparable molecular anisotropy, $\Delta R_{VV}/HMC$ should extrapolate to the same intercept in the absence of molecular aggregation

To account for the absorption, the extinction coefficient ν(cm^2 g^{-1}) was determined according to equation (19). *Figure 4* shows plots of $\ln(1/\gamma)$ vs. concentration with $\nu = 1.7\times10^2$ g^{-1} and 6.3×10 cm^2 g^{-1} for $\lambda_0 = 488$ and 632.8 nm, respectively. At low concentrations ($C \lesssim 1\times10^{-3}$ g cm^{-3}), only substantial errors in ν contribute towards the absorption correction (as in equation (19)) in the scattered intensity. Therefore, it is acceptable to measure an apparent extinction coefficient to correct for the attenuation effect produced by the absorption of light both in the incident beam in reaching the scattering volume from the entrance at the light-scattering cell wall and in the scattered beam in traversing from the scattering volume to the light-scattering cell wall. In this case, the total path length d is 8 mm with $I_s = I_{s,apparent} e^{\nu C d}$. At $\lambda_0 =$ 488 nm and $C \approx 10^{-3}$ g cm^{-3}, an attenuation correction of the order of 15% is needed. In addition to the absorption problem, the PPTA solution also fluoresces. So, in the light scattering spectrometer, a narrow-band interference filter was inserted before the photomultiplier tube to essentially exclude the fluorescence intensity.

Preliminary results at incident wavelengths $\lambda_0 = 488$ and 632.8 nm with respective interference filters, again show reproducible results indicating that meaningful light-scattering measurements could be made for fluorescent systems. *Figure 5* shows a plot of $\Delta R_{VV}/HC$ vs. concentration for sample 5. According to equations (6) and (9), the intercept yields an apparent molecular weight M_{app} which is related to M_w by the relation $M_{app} = M_w(1 + 4/5\delta^2)$. With the molecular anisotropy remaining relatively constant, the slight variation in the intercept suggests variation of the molecular weight of PPTA in 96% H_2SO_4. The values of M_w are listed in *Table 1*. M_w again appears to approach a relatively constant value at 96% H_2SO_4 + 0.05 M K_2SO_4.

It should also be noted that the slope of the curve changes sign at higher concentrations signifying that in molecular weight determinations we must make light-scattering measurements at low concentrations ($C \lesssim 10^{-3}$ g cm^{-3} for PPTA sample 5). Extrapolation of $\lim_{K\to 0}\Delta R_{VV}/HC$ to finite dilution from intensity measurements at higher concentrations ($C \gtrsim 3\times 10^{-3}$ g cm^{-3} for PPTA sample 5) could lead to erroneous conclusions.

To emphasize this point, we show an additional plot of $\Delta R_{VV}/HMC$ as a function of concentration for PPTA sample 4. In *Figure 6*, we have noted that PPTA has a slightly higher molecular weight ($M_w \simeq 3.8\times10^4$ g mol^{-1}) when it is dissolved in 96% H_2SO_4; but the molecular weight is decreased to a constant value ($M_w \simeq 3.0\times$

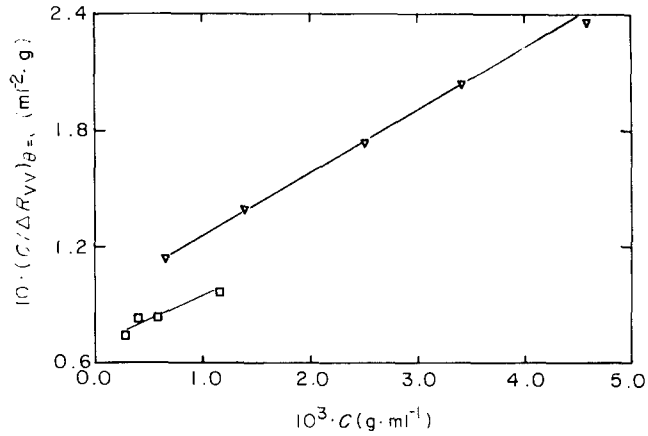

Figure 7 Plots of $(C/\Delta R_{VV})_{\theta=0}$ vs. concentration for samples 4 (▽) and 5 (□) in 96% H_2SO_4 + 0.005 M K_2SO_4. $(\Delta R_{VV})_{\theta=0} \lim_{K\to 0} Rvv$ with △ stressing excess Rayleigh ratio

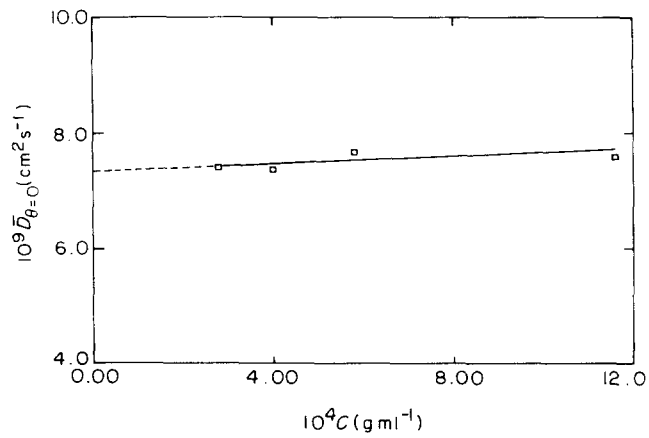

Figure 8 Plot of $\bar{D}_{\theta=0}$ vs. concentration at 30°C for sample 5. $\bar{D}_z = 7.15\times10^{-9}(1 + 60C)$ cm^2 s^{-1} with C expressed in g cm^{-3}

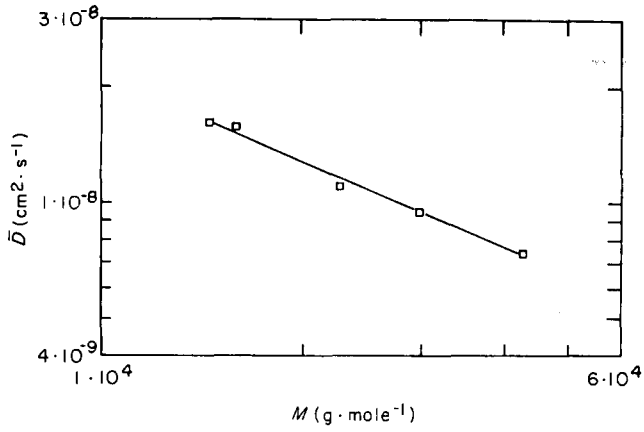

Figure 9 Log–log plot of $\bar{D}$ vs. M at 30C where $\bar{D}$ and M denote the z-average translational diffusion coefficient at infinite dilution and the weight average molecular weight M_w. According to equation (18), $\bar{D} = 2.11 \times 10^{-5} M^{-0.749}\,cm^2\,s^{-1}$ with M expressed in units of g mol^{-1}

10^4 g mol^{-1}) using 96% H_2SO_4 plus a small amount of added salt (0.005 and 0.05 M K_2SO_4) as shown by the results listed in *Table 1*. In addition, the lower molecular weight for sample 4 extends the dilute solution region to a slightly higher concentration. Nevertheless, the same precaution must be exercised in extrapolating $\Delta R_{VV}/HC$ to zero concentration and in determining the initial slope for A_2. Estimates of A_2 are listed in *Table 1* for the five PPTA samples using plots of $(C/\Delta R_{VV})_{\theta=0}$ vs. concentration as shown in *Figure 7*.

From linewidth measurements, the translational diffusion coefficient is related to the linewidth by the relation $\Gamma = DK^2$. For a polydisperse system, $\bar{\Gamma} = \langle D \rangle_z K^2$ where:

$$\langle D \rangle_z = \sum N_i M_i^2 D_i / \sum N_i M_i^2 \qquad (20)$$

with N_i and M_i being the number and molecular weight of ith species. However, at finite scattering angles:

$$\bar{D}_\theta = \sum N_i M_i^2 P_i(K) D_i / \sum N_i M_i^2 P_i(K) \qquad (21)$$

where $P_i(K)$ is the particle scattering factor for the ith species at K. Then, to determine $\bar{D}_z (\equiv \langle D \rangle_z)$, we need to extrapolate $\bar{D}_\theta$ to zero scattering angle so that $\bar{D}_z = \bar{D}_{\theta=0}$. This precautionary measure becomes important whenever $P(K)$ becomes appreciable. In particular, when there is fairly broad distribution of sizes as denoted by the magnitude of $\mu_2/\bar{\Gamma}^2$, $\bar{D}_\theta$ should be extrapolated to zero scattering angle. *Figure 8* shows a typical plot of $\bar{D}_{\theta=0}$ as a function of concentration for sample 5. With:

$$\bar{D}_z = \bar{D}_z^0 (1 + k_d C), \qquad (22)$$

we have $\bar{D}_z^0 (\equiv \langle D \rangle_{z,0}) = 7.15 \times 10^{-9}\,cm^2\,s^{-1}$ and $k_d = 60\,cm^3\,g^{-1}$. At $C \approx 3 \times 10^{-4}\,g\,cm^{-3}$, the concentration effect corresponds to a 0.018 (or $\approx 2\%$) correction according to equation (22). Therefore, the concentration effect can essentially be taken into account even if k_d depends on molecular weight. In the second paper dealing with the molecular weight distribution transform, we do approximate k_d to be independent of molecular weight and the error introduced by this approximation becomes negligible at low concentrations since the total effect amounts to only a few per cent. There is a problem associated with signal-to-noise optimization in the determination of molecular weight distribution, i.e., linewidth measurements should be made at sufficiently high concentrations to improve the signal-to-noise ratio, but not so high that the approximation for k_d to be independent of molecular weight becomes appreciable. Measurements should therefore be performed essentially in dilute solutions. *Figure 9* shows a log–log plot of $\bar{D}_z^0$ vs. M. A least squares fitting of the five data points yields $\bar{D}_z^0 = 2.11 \times 10^{-5} M^{-0.749}\,cm^2\,s^{-1}$ for PPTA in 96% H_2SO_4 + 0.05 M K_2SO_4. The value of the scaling exponent $\alpha_D = 0.749$ which is greater than 0.5 and ≈ 0.6 for polymer coils in a theta solvent and a good solvent, respectively. Over relatively small molecular weight ranges, equation (18) is valid and yields an effective scaling exponent which clearly shows PPTA to have worm-like-chain behaviour. We have collected all the known intrinsic viscosity data and made a log–log plot of $[\eta]$ vs. molecular weight for PPTA in 96% H_2SO_4. Over a limited molecular weight range, we can express the molecular weight dependence of intrinsic viscosity by an expression:

$$[\eta] = k_\eta M^{a_\eta} \qquad (23)$$

which is similar to equation (18). A least-squares fitting of all the published intrinsic viscosity data over a molecular weight range of $5 \times 10^3 \lesssim M \lesssim 10^5$ yields $k_\eta = 1.09 \times 10^{-3}$

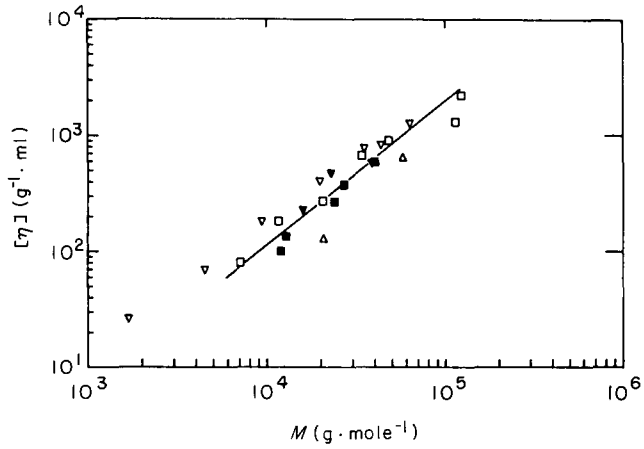

Figure 10 Log–log plot of $[\eta]$ vs. molecular weight for PPTA in 96% H_2SO_4 at 30°C. ■, Results from reference 27; ▼, this work (Institute of Chemistry, Beijing); ▽, reference 25; □, reference 26; △ reference 5. $[\eta] = 1.09 \times 10^{-3}\,M^{1.25}$ with $[\eta]$ and M expressed in ml g^{-1} and g mol^{-1}

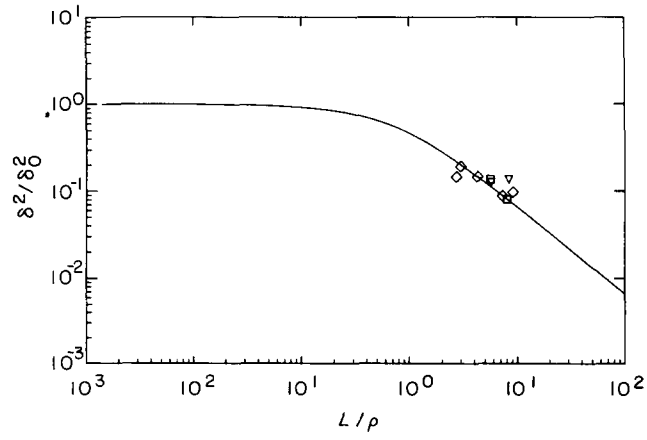

Figure 11 Ratio of square of overall molecular anisotropy to segment anisotropy $(\delta/\delta_0)^2$ as a function of L/ρ. ——, $(\delta/\delta_0)^2$ vs. L/ρ according to equations (11) and (12); △, five PPTA fractions in 96% H_2SO_4; □, samples 4 and 5 in 96% H_2SO_4 + 0.005 M H_2SO_4; ▽, samples 4 and 5 in 96% H_2SO_4 + 0.05 M K_2SO_4. All δ and M_w values are listed in *Table 1*. In the plot, $\delta_0 \sim 0.7$ has been assumed

and $\alpha_\eta = 1.25$ with $[\eta]$ and M expressed in units of ml g^{-1} and g mol^{-1}, respectively. It is remarkable that the values of α_η and α_D obey the relation $3\alpha_D - 1 = \alpha_\eta$ even though the intrinsic viscosity data were determined in 96% H_2SO_4 while the diffusion coefficient data were measured in 96% H_2SO_4 + 0.05 M K_2SO_4. The agreement suggests that PPTA has worm-like-chain behaviour in 96% H_2SO_4 with or without added salt. On the other hand, the published intrinsic viscosity data were quite scattered. There is no *a priori* reason to accept the value of α_η as reliable. A comparison of diffusion coefficient results with $[\eta]$ merely supports the diffusion coefficient measurements and analysis. *Figure 9* can be used to convert hydrodynamic size distribution to the molecular weight distribution without introducing any arbitrary parameters.

According to equations (11) and (12), as shown by the solid curve in *Figure 11*, we can determine the persistence length, ρ, if we know $(\delta/\delta_0)^2$ and the molecular weight M since the contour length $L = lM/M_L$Å with the segment length[28] $l = 12.9$ Å and the mass per segment M_L being 238 g. If we take $\delta_0 = 0.7$, the experimental results show $\rho \sim 2.9 \times 10^2$ Å which appears to be in fairly good agreement with the literature value[29] of $\rho \approx 200 \pm 50$ Å.

CONCLUSIONS

When PPTA is dissolved in 96% sulphuric acid, it becomes protonated. Long-range electrostatic interactions for such macro-ions are likely to be in delicate balance with the counter ions. From there molecular weight determinations by means of light scattering measurements it can be seen that the presence of a small amount of molecular aggregates for PPTA in 96% H_2SO_4 can be suppressed by addition of potassium sulphate. Note that both the intrinsic viscosity and the molecular weight of PPTA appear to approach a constant low value for PPTA in 96% H_2SO_4 with 0.05 M K_2SO_4. Furthermore, from estimates of $\mu_2/\bar{\Gamma}^2$ and equation (18), the width of the size distribution is in reasonable agreement with the expected polydispersity of PPTA for such polycondensation reactions. A more detailed analysis of the characteristic linewidth distribution function, $G(\Gamma)$, to be presented in the second paper, also shows an absence of bimodality suggesting negligible amounts of molecular aggregates. Thus, we are reasonably certain that we have been able to determine the molecular weight of essentially unaggregated PPTA in solution.

96% sulphuric acid has a fairly high ionic strength. In the presence of added salt, the long range electrostatic effect has been shielded. Thus, we do not expect to observe slow macroscopic dynamics from such PPTA solutions. *Figures7* and *8* show linear concentration dependence.

In summary, we have been able:

1. to overcome the absorption of light by the PPTA solution using measurements of different incident wavelengths ($\lambda_0 = 632.8$ and 488 nm) and power; to correct for the attenuation of integrated light-scattering intensity by independently determining the extinction coefficient ν;
2. to examine the effects of fluoroescence by using different incident wavelengths ($\lambda_0 = 632.8$ and 488 nm); to essentially eliminate the fluorescence intensity by inserting a narrow-band interference filter in front of the photomultiplier tube;
3. to avoid (or reduce) aggregation and long-range electrostatic interactions by adding a small amount of salt (K_2SO_4);
4. to devise an acceptable procedure for solution clarification without invoking the use of filters which are often unsuitable for clarification of worm-like chains in polar solvents; and
5. to take into account the molecular anisotropy by measuring both R_{VV} and R_{HV}. With the establishment of reasonable procedures and knowing the magnitude of equation (18), it is possible to determine the molecular weight distribution of PPTA by means of laser light scattering and correlation function profile analysis.

ACKNOWLEDGEMENT

The authors gratefully acknowledge support of this research by the National Science Foundation, INT 8211992 and Polymers Program (DMR 8314193).

REFERENCES

1 Blades, H. US Pat. 3,767,756, 1973 and 3,869,429, 1975
2 Kikuchi, J. *J. Textile Mach. Soc. Jpn.* 1974, **27**, 722
3 Kevlar is a DuPont registered trademark for its family of aramid fibres
4 Chu, B., Ying, Q.-C., Wu, C., Ford, J. R., Dhadwal, H., Qian, R.-Y., Bao, J.-S., Zhang, J.-Y. and Xu, C.-C. *Polymer* 1984, **25**, (*Commun*), 211
5 Wong, C.-P., Ohnuma, H. and Berry, G. C. *J. Polym. Sci. Polym. Symp.* 1978, **65**, 173
6 Metzger-Cotts, P. and Berry, G. C. *J. Polym. Sci. Polym. Phys. Ed.* 1983, **21**, 1255; and references therein
7 Lee, C. C., Chu, S.-G. and Berry, G. C. *J. Polym. Sci. Polym. Phys. Ed.* 1983, **21**, 1573; and references therein
8 Berry, G. C. *Discuss. Faraday Soc.* 1970, **99**, 121; *J. Polym. Sci. Polym. Symp.* 1978, **65**, 143
9 Helminiak, T. E. and Berry, G. C. *J. Polym. Sci. Polym. Symp.* 1978, **65**, 107
10 Chu, S.-G., Venkatraman, S., Berry, G. C. and Einaga, Y. *Macromolecules* 1981, **14**, 939
11 Berry, G. C., Metzger-Cotts, P. and Chu, S.-G. *Br. Polym. J.* 1981, **13**, 47
12 Einaga, Y. and Berry, G. C. 'Studies on Dilute Solutions of Rod-like Macroions III. Integrated Intensity and Photon Correlation Light Scattering Investigation of Association', preprint
13 Schaefgen, J. R., Foldi, V. S., Logullo, F. M., Good, V. H., Gulrich, L. W. and Killian, F. L. *Polym. Am. Chem. Soc. Div. Polym. Chem.* 1969, **17**, 69
14 Yamakawa, H. 'Theory of Polymer Solutions', Harper and Row, New York, 1971
15 Yamakawa, H. and Stockmayer, W. H. *J. Chem. Phys.* 1972, **57**, 2843
16 Yamakawa, H. and Fujii, M. *Macromolecules* 1973, **6**, 407; 1974, **7**, 128
17 Nagai, K. *Polym. J.* 1972, **3**, 67
18 Benoit, H. *C.R. Acad. Sci.* 1953, **236**, 687
19 Koppel, D. E. *J. Chem. Phys.* 1972, **57**, 4814
20 Ford, J. R. and Chu, B. in 'Proceedings of the 5th International Conference on Photon Correlation Techniques in Fluid Mechanics', Springer-Verlag, NY, 1983, pp. 303–314
21 Lawson, C. L. and Hanson, R. J. 'Solving Least Squares Problems', Prentice-Hall, New Jersey, 1974
22 Chu, B., Ford, J. R. and Dhadwal, H. S. 'Correlation Function Profile Analysis of Polydisperse Macromolecular Solutions and Colloidal Suspensions', in *Methods of Enzymology*, to be published
23 Bao, J.-S., You, A.-J., Zhang, S.-Q., Zhang, S.-F. and Hu, C. *J. Appl. Polym. Sci.* 1981, **26**, 1211
24 DiNapoli, A., Chu, B. and Cha, C. *Macromolecules* 1982, **15**, 1174
25 Arpin, M. and Strazielle, C. *C.R. Acad. Sci. Sev. C* 1975, **280**, 1293
26 Schaefgen, J. R., Foldi, V. A., Logullo, E. M., Good, V. H., Gulrich, L. W. and Killian, F. L. *Polym. Am. Chem. Soc. Div. Polym. Chem.* 1969, **17**, 69
27 Baird, D. G. and Smith, J. K. *J. Polym. Sci. Polym. Chem. Ed.* 1978, **16**, 61
28 Northolt, M. G. *Eur. Polym. J.* 1974, **10**, 799
29 Arpin, M. and Strazielle, C. *Polymer* 1977, **18**, 591